Food Chemistry: X 25 (2025) 102160

Contents lists available at ScienceDirect

Food Chemistry: X

journal homepage: www.sciencedirect.com/journal/food-chemistry-x

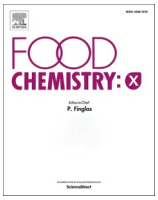

Exploring the noncovalent interaction between β-lactoglobulin and flavonoids under nonthermal process: Characterization, physicochemical properties, and potential for lycopene delivering

Gongshuai Song, Fang Li, Ziming Xu, Nengliang Jiang, Danli Wang, Tinglan Yuan, Ling Li, Jinyan Gong *

Zhejiang Provincial Key Lab for Biological and Chemical Processing Technologies of Farm Product, School of Biological and Chemical Engineering, Zhejiang University of Science and Technology, Hangzhou 310023, Zhejiang, China

ARTICLE INFO

Keywords:
Lycopene
Flavonoids
β-Lactoglobulin
Noncovalent interaction
Ultrasound

ABSTRACT

The poor structure stability and low bioavailability of lycopene (LY) hampers the wide application in food field. Thus, it is crucial to explore novel deliver carrier for LY based on protein-flavonoid complexes. In this study, the noncovalent interaction mechanism between β-lactoglobulin (β-LG) and flavonoids (apigenin (API), luteolin (LUT), myricetin (MY), apigenin-7-O-glucoside, luteolin-7-O-glucoside, and myricetrin) under ultrasound treatment was explored. Results revealed that ultrasound treatment promoted reactive groups exposure and structural unfolding of β-LG to interact with six flavonoids. The main driving force between β-LG and flavonoids was hydrophobic interaction. The docking result showed that the preferred binding site for these flavonoids was on the outer surface of β-LG. The thermal stability, surface hydrophilicity, and antioxidant properties of β-LG-API, β-LG-LUT, and β-LG-MY complexes were superior by multi-spectroscopy methods and molecular simulation analysis ($P < 0.05$). The ability of β-LG-API for delivering LY was the best among above three binary complexes, revealing superior environmental stability and bioavailability of the β-LG-API-LY complex. This study will help to understand the ultrasound-assisted noncovalent binding of protein-flavonoid complexes, and exhibit the potential as a novel delivery system for delivery and protection of LY.

1. Introduction

Dietary flavonoids are widely distributed in nuts, vegetables, cereal grains, fruits, and etc., which are natural bioactive agents and classified into some subclasses (e.g., flavonols, anthocyanidins, flavanones, isoflavones, chalcones, and flavones) with a common C6-C3-C6 skeleton based on their chemical structures (Jia et al., 2022). It has been reported that dietary flavonoids possess a broad spectrum of health-beneficial effects because of the powerful antioxidant activity. It is an effective way that dietary ingestion of a great deal of flavonoids to reduce the risk of many diseases (e.g. anticancer, anti-inflammatory, antibacterial, antioxidant, and scavenging free radicals) (Jin et al., 2024; Liang et al., 2023; Shen et al., 2022). Apigenin (API) is a natural flavone, which is abundant in the chamomile plant. Due to its multiple health benefits by acting as an antioxidant agent and directly targeting many human cellular targets, API is becoming popular increasing as a functional food ingredient (Zhu et al., 2020). Apigenin-7-O-glucoside (AGL) can be found in medicinal plants (e.g., Scutellaria baicalensis, chamomile, and plantain), which is a glycosylated derivative of API. Zhao et al. found that AGL can also enhance the expression of antioxidant enzymes in cancer and Alzheimer's disease, and scavenge free radicals like API (Zhao et al., 2024). Luteolin (LUT) and luteolin-7-O-glucoside (LGL) belong to flavonoid aglycones, which are rich in the flower of *Dendranthema morifolium*. It has been demonstrated that the biological activities of LUT and LGL are associated with the antiallergic activities, antitumorigenic effects, and antioxidant potential (Lin et al., 2015). Myricetin (MY) and myricetrin (MYR) are viewed as the main flavone compounds in *Myrica rubra* that is a plant with high medicinal value. These two compounds have exhibited many beneficial effects (e.g., anticarcinogenic, antioxidant, antimicrobial, and anti-inflammatory effects) (Li et al., 2021). However, one of the significant hampers for the utilization of these dietary flavonoids with promising therapeutic value and nutraceutical benefits is the low bioavailability because of poor solubility in nonpolar solvents and water, and rapid metabolism

* Corresponding author.
E-mail address: jygong@zust.edu.cn (J. Gong).

https://doi.org/10.1016/j.fochx.2025.102160
Received 28 October 2024; Received in revised form 28 December 2024; Accepted 3 January 2025
Available online 10 January 2025

elimination when administered orally (Meng et al., 2023).

Several strategies (e.g., hydrogel beads, microcapsule, and emulsion) have been developed to enhance the bioactivity of these dietary flavonoids to facilitate their utilization in functional food field (Liang et al., 2023). It has been demonstrated that binding between proteins and flavonoids can improve the bioactivity, bioavailability, solubility, and stability of flavonoids. In addition, the structure and function (e.g., solubility, emulsifying and foaming properties) of proteins can be modified by interacted with flavonoids (Liu et al., 2023). Flavonoids can bind to proteins covalently or non-covalently. However, Zhang et al. found that the undesired by-products such as quinone can be often formed during the covalent binding process. The biological activity and stability of flavonoids may be decreased under high-temperature and alkaline conditions (Zhang, Li, et al., 2021). It is meaningful to decipher the characteristic and noncovalent interaction mechanism between protein molecules and flavonoids.

β-Lactoglobulin (β-LG) is a key component of whey protein (Song et al., 2025). β-LG comprises 162 amino acid residues with a molecular weight of 18.3 kDa. Its secondary structure consists of nine β-strands and one α-helix, with strand A-H forming a conical β-barrel called a calyx. The ninth strand (strand I) plays a significant part in the dimer interface and is key in dimer interactions (Shafaei et al., 2017). Thus, β-LG can be employed as a transport vector for various compounds due to its unique secondary structural properties, which enable it to bind to different amphiphilic and hydrophobic ligands. Recently, it has drawn widespread attention that the potential utilization of β-LG as a carrier for flavonoids because of its several hydrophobic cavities. Song et al. revealed that hydrophobic cavities can affect the bind rate between proteins and flavonoids (Song, Zeng, et al., 2024). It is essential to expose more binding sites of β-LG. Ultrasound technique has been used in many food processing fields, which is a non-thermal technique. Cavitation bubbles and microstreaming currents can be generated by the shear stress and high mechanical energy during high-intensity ultrasound process (ca. 20–100 kHz). The physicochemical property of food components can be modified by ultrasound treatment, which has been used to enhance the efficiency of various food processing methods such as extraction, freezing/thawing, homogenization/emulsification, and filtration (Song et al., 2025). Characterization of the noncovalent interaction mechanism between β-LG and flavonoids under ultrasound is complicated. To explore the interaction mechanism is the prerequisite for the application of β-LG-flavonoid complexes. Lycopene (LY) is a sort of lipophilic natural unsaturated carotenoid, which is abundant in watermelon, guava, tomato, and other red fruits (Zhu et al., 2024). Nowadays, LY is widely applied to develop functional foods, pharmaceuticals, and cosmetic products because of the superb bioactivities such as delaying senescence, protecting cardiovascular system, and retarding atherosclerosis (Wang et al., 2021). However, LY is susceptible to oxidative degradation and isomerization due to the presence of eleven conjugated double bonds and two non-conjugated double bonds. It is essential to design appropriate delivery systems to improve the bioavailability and stability of LY.

In this study, the potential effect of ultrasound treatment on noncovalent interactions between β-LG and three flavonoids (API, LUT, and MY) and their corresponding glycosylated derivatives (AGL, LGL, and MYR) was investigated. The structural and conformational variations of β-LG after these flavonoids binding and the molecular basis underlying noncovalent interactions during ultrasound treatment were explored by multi-spectroscopy methods, namely, fluorescence spectrometry, Fourier infrared spectroscopy (FTIR), circular dichroism (CD), differential scanning calorimetry (DSC), in combination with the computational analysis method (molecular docking simulation). Then three fabricated β-LG–flavonoid complexes were used as the carrier to deliver LY. The bioavailability of β-LG–flavonoid-LY complexes was also studied.

2. Materials and methods

2.1. Materials and reagents

β-LG (molecular weight 18.4 kDa, purity ≥95 %, from milk) and LY (molecular weight 536.88, purity ≥90 %) were bought from Macklin Biochemical Co., Ltd. (Shanghai, China). 8-Anilino-1-naphthalenesulfonic acid ammonium salt (ANS-Na) for fluorescence, API (molecular weight 270.24, purity ≥97 %), AGL (molecular weight 432.38, purity ≥98 %), LUT (molecular weight 286.24, purity ≥98 %), LGL (molecular weight 448.38, purity ≥98 %), MY (molecular weight 318.24, purity ≥98 %), and MYR (molecular weight 464.38, purity ≥98 %) were all provided by Sigma-Aldrich Chemical Company (St. Louis, MO, USA). Other reagents with analytical grade were provided by Sinopharm Chemical Reagent Co., Ltd. (Shanghai, China). Ultra-pure deionized water used for all experiments was filtered by Millipore Milli-Q system (Millipore, Bedford, MA, USA).

2.2. Preparation of complexes

The ultrasound-assisted noncovalent β-LG-flavonoid complexes were prepared according to the reported method of Liu et al. (2022) with some minor modifications (Liu et al., 2022). β-LG powders (1 g) were dissolved in deionized water (50 mL), which was stirred for 2 h gently at room temperature. Then, the β-LG solution was processed for 15 min by ultrasound treatment (25 °C, 400 W) using a SCIENTZ JY92-IIDN ultrasound homogenizer (Shanghai Puyukemao Co., Ltd., Shanghai, China) (Li et al., 2016). The flavonoids were dissolved in a suitable volume of ethanol and subsequently diluted to 50 mL with deionized water, resulting in a final concentration of 0.35 mM. And the Flavonoid solutions were added to above β-LG solution, respectively. After reacted at room temperature for 24 h, the complexes were dialyzed with dialysis membranes (3500 Da) in deionized water at pH 7 for 48 h. The dialysate was then stored at 4 °C, with water changes every 6 h to dialyze out unbound flavonoids. And then the dialysate was pre-frozen and vacuum lyophilized for 48 h. The obtained complex was stored at −20 °C until use.

2.3. Determination of binding capacity

Referring to the previous study, the binding capacity between β-LG and flavonoids was determined (Wang et al., 2022). In brief, 0.5 mL of the β-LG-flavonoid complex (1 mg/mL) was mixed with 0.5 mL of Folin-Ciocalteu reagent for 3 min. Afterwards, 2 mL of 20 % sodium carbonate was added. The mixed solution was vortexed and incubated at 25 °C for 2 h in the darkness. Using an ultraviolet spectrophotometer (UV2600, Shimadzu, Japan) at a wavelength of 760 nm, the absorbance was measured. Deionized water was used as the control solution for absorbance measurement. Results are expressed as nmol/mg.

2.4. Structural characteristics

2.4.1. Scanning electron microscopy (SEM)

The measurement of scanning electron microscopy (SEM) was carried out. In brief, samples were frozen at −20 °C overnight and then lyophilized using a freeze drier (ALPHA 1–2, CHRIST, Osterode, Germany). Powered mixtures were coated with a layer of gold metal under high vacuum and observed by a SEM (QUANTA 250 FEG, Thermo Fisher Scientific, U.S.) at 20.0 kV (Liu et al., 2022).

2.4.2. Particle size and zeta potential

Using a laser particle sizer (Malvern Instruments, Ltd., Malvern, UK), the average particle size, polydispersity index (PDI), and zeta potential of samples were carried out referring to the previous method with slight modifications (Song, Zeng, et al., 2024).

2.4.3. X-ray diffractometry (XRD)

The crystalline structure was performed by an XRD diffractometer (Smartlab9, Rigaku, Japan) with Cu-Kα X-ray radiation (λ = 1.5406 nm). XRD spectra were recorded in range of 2θ = 5–35° (Gu et al., 2023).

2.4.4. FTIR spectroscopy

FTIR of samples was carried out by potassium bromide (KBr) compression method using a spectrophotometer (Nicolet 5700, Thermo Electron Co., Waltham, MA, USA). The spectral range, number of scans, and resolution were set as 4000–400 cm^{-1}, 32, and 4 cm^{-1}, respectively. KBr was used as a blank control (Gao et al., 2023).

2.4.5. Fluorescence spectroscopy

The intrinsic fluorescence of samples was measured at 303 K using a fluorescence spectrophotometer (Hitachi Ltd., Tokyo, Japan). Samples were diluted to 10 mL with phosphate buffer (PBS, pH 7.2, 10 mM). The scanning speed was set at 1200 nm/min, the emission wavelength was set at 300–400 nm, and the excitation wavelength was set at 280 nm. The width of the slit was set to 5 nm, and the PBS was used as a blank control (Zhu et al., 2020).

2.4.6. CD spectroscopy

A CD spectrometer (Brighttime Chirascan, Applied Photophysics, UK) was applied to record CD spectroscopy in the 190–300 nm wavelength range at room temperature. Samples were reconstituted into PBS (pH 7.2, 10 mM). Using the online Dichroweb program (University of London, UK), the fraction of secondary structure (α-helix, β-sheet, β-turn, and random coil) was computed (Gao et al., 2023).

2.4.7. Molecular docking

The binding modes between β-LG (PDB ID:3NPO) and API (molecular weight 270.24, purity ≥97 %), AGL (molecular weight 432.38, purity ≥98 %), LUT (molecular weight 286.24, purity ≥98 %), LGL (molecular weight 448.38, purity ≥98 %), MY (molecular weight 318.24, purity ≥98 %), and MYR (molecular weight 464.38, purity ≥98 %) were established by AutoDock Vina 1.1.2 software. The API, AGL, LUT, LGL, MY, and MYR molecule could be obtained from the ZINC database (http://zinc.docking.org/), and the β-LG crystal could be downloaded from the Research Collaboratory for Structural Bioinformatics Protein Data Bank (http://www.rcsb.org). Using PyMol 2.5 and Maestro 12.9, docking results were visualized and analyzed (Zhang, Lu, et al., 2021).

2.5. Functional properties

2.5.1. Determination of thermal stability

The thermal stability of samples was analyzed using a Q20 DSC (TA Instruments, Inc., New Castle, DE, USA) as previously reported (Song et al., 2025). In briefly, 5 mg sample was placed in a lead sample tray and sealed aluminum pan. The heating rate, the range of heating temperature, and flow rate of nitrogen were set as 10 °C/min, 30 °C–180 °C, and 30 mL/min, respectively. Based on the corresponding thermal curves, the denaturation temperature (Td, °C) and enthalpy values (ΔH, J/g protein) were calculated.

2.5.2. Determination of surface hydrophobicity

The surface hydrophobicity of the samples was assessed using the ANS fluorescent probe method (Wu et al., 2021). In brief, ANS solutions (8 mM) was prepared with the PBS (10 mM, pH = 7.0). Samples were diluted to concentrations of 0.02, 0.05, 0.10, 0.20, and 0.30 M using the PBS (10 mM, pH = 7.0), respectively. After incubation in the darkness at 25 °C for 10 min, the fluorescence intensity at 390 nm (excitation wavelength) and 470 nm (emission wavelength) was measured, respectively.

2.5.3. Antioxidant properties

The antioxidant property of samples was evaluated by the measurement of the free radical (DPPH· and $ABTS^{\cdot+}$) scavenging activity, and ferrous irons chelating activity (FRAP) as previously described (Song, Zeng, et al., 2024).

2.6. Preparation of LY loaded complexes

According to the previous method, three LY loaded β-LG-flavonoid complexes were prepared (Wang et al., 2021). In a light-proof centrifugal tube with anhydrous ethanol, the LY solution (2 mM) was prepared. The β-LG-flavonoids (API, LUT, and MY) complexes were redissolved, respectively. For full hydration, all solutions were mixed at room temperature for 1 h and stored at 4 °C overnight. The β-LG-flavonoids-LY complexes were prepared with low ethanol concentration (≤ 3 %), ensuring no appreciable ethanol-induced protein denaturation. Finally, the embedding rate of lycopene in the samples was determined according to the method of Li et al. (Li et al., 2021).

2.7. The stability of the complex

According to previous methods with slight modifications, the stability characteristics mainly including pH stability, thermal stability, SSF centrifugal stability, freezing stability and light stability were analyzed (Song et al., 2025; Zhao et al., 2024).

2.8. In vitro gastrointestinal digestion

The standardized in vitro simulated digestion model was built by configuring simulated saliva (SSF), simulated gastric fluid (SGF), and simulated intestinal fluid (SIF) according to the reported method (Song et al., 2025).

2.9. Statistical analysis

All experiments were conducted three times and data were statistically analyzed using SPSS 26.0 (SPSS Inc., Chicago, IL, USA) with the analysis of variance (ANOVA, $p < 0.05$) using Duncan's method and graphs using Origin 2021 (Song, Guo, et al., 2024; Song, Zhou, et al., 2024).

3. Results and discussion

3.1. Binding capacity

According to the structure, polyphenols are classified as non-flavonoids and flavonoids. As shown in Fig. 1A, API, LUT, and MY belong to flavonoids, which contain two aromatic groups and one oxygen-containing heterocyclic group (Guan et al., 2021). Their corresponding glycosylated derivatives differ greatly in the chemical struture because of the degree of glycosylation as shown in Fig. 1A. In this study, API, LUT, MY and their corresponding glycosylated derivatives were selected because these compounds have been demonstrated to possess the capacity to enhance the expression of antioxidant enzymes in conditions (e.g., cancer, diabetes, and Alzheimer's disease), and scavenge free radicals. The ability of β-LG to bind these flavonoids was determined according to the previous method (Fig. 1B). After ultrasonic treatment, the flavonoid content of each sample increased, which may be due to the shear effect of ultrasound. It can destroy the structure of the protein and expose its binding site. Among them, the binding amount of β-LG and MY was the largest (22.6 nmol/mg), mainly because the number of phenolic hydroxyl groups contained in MY is the largest. It has been revealed that the number and location of phenolic hydroxyl groups can affect the interaction between proteins and polyphenols significantly (Pan et al., 2023). Kanakis et al. reported that the more hydroxyl groups can favor the more binding of β-LG and polyphenols (Kanakis et al., 2011). The binding equivalent of MYR to β-LG is 13.43 nmol/mg was lower than that of MY. The decrease in the binding ability

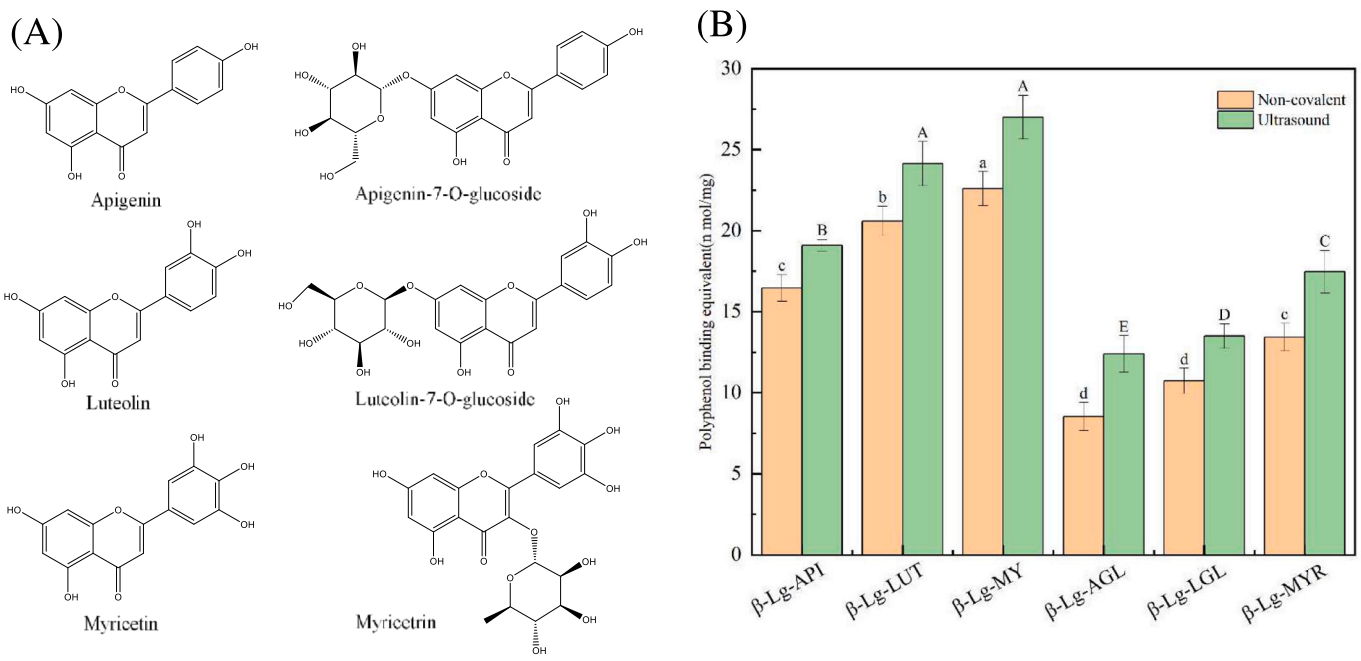

Fig. 1. (A) Chemical structures of flavonoids and corresponding glycosylated derivatives; (B) Binding capacity between β-LG and flavonoids.

of β-LG and MYR after glycosylation reaction may be due to the increase in the size and polarity of MYR molecule, and the decrease in hydroxyl groups replaced by glycosylated groups, which makes it transform into a non-plane structure, and enlarge steric hindrance (Fu et al., 2023). In addition, glycosylation may reduce the hydrophobicity of the compound. It has been demonstrated that the hydrophobic interaction force plays an important role in the binding of flavonoids to proteins (Alizadeh-Pasdar & Li-Chan, 2000). Wang et al. also found that the binding ability of pea protein isolate to hesperitin and naringenin was stronger than that of hesperidin and naringin (Wang et al., 2024).

3.2. Changes in microstructure, particle size and zeta potential

The microscopic morphology of β-LG-flavonoid binary complexes can be observed by SEM. As shown in Fig. 2, β-LG usually presents an irregular spherical shape with concave depression. After ultrasound, the structure of β-LG was destroyed. It could be seen that the large piece of lamellar structure disappeared, and the edge of the broken small pieces was smooth. The collapse of bubbles and shear force could be generated due to the shock wave of ultrasound, which destroyed the protein structure. In addition, the previous literature reported that the prolonged ultrasonic treatment may make the loose structure of β-LG reaggregate together, causing macromolecular protein recombine and forming new aggregated structure (Leong et al., 2017). The stability of β-LG could enhance after binding to flavonoids by non-covalent interactions (e.g., hydrogen bonds, hydrophobic interactions, and van der Waals forces) (Zhang et al., 2022). The structures of β-LG-API and β-Lg-LUT complexes were mostly sheet-like with less honeycomb structure. After glycosylation reaction, β-LG-AGL and β-LG-LGL complexes were diverse in shape with rod-like or spherical structures and loose texture, which may weaken the intermolecular and intramolecular interaction. The structures of β-LG-My and β-LG-MYR were compact, lamellar and uniform in texture. Results of changes in structures of β-LG-flavonoid complexes before and after ultrasound were similar with that of β-LG.

The particle size and potential of samples were determined by a Malvern particle size analyzer, the result was depicted in Fig. 3. Compared with β-LG, the particle size of complexes increased after binding flavonoids (Fig. 3A), After ultrasound treatment, the particle size of the complex decreased (Fig. 3B). This may be due to the shear and cavitation effects of ultrasound, which can destroy the interaction between proteins and flavonoids, and reduce the particle size of the complex (Song, Zeng, et al., 2024). As depicted in Fig. 3C and D, the zeta potential values of β-LG and β-LG-flavonoids complexes were all negative. It could be explained that the hydrophilic group was exposed on the surface of the protein when dissolved in the aqueous solution, resulting in a partial charge on the protein surface. After ultrasonic treatment, the absolute zeta potential values of samples increased, indicating that ultrasonic treatment could promote the molecular unfolding of proteins and increase the interaction between molecules (Liu et al., 2022).

3.3. Conformational structural modifications

FTIR is commonly used to determine the secondary structure of proteins. The spectrum of the protein is generally divided into three parts: amide A band (3300–3600 cm^{-1}), amide I band (1600–1700 cm^{-1}), and amide II band (1500–1600 cm^{-1}). As shown in Fig. 4A, the characteristic absorption peaks of β-LG in the amide A band, amide I band, and amide II band were 3293.3 cm^{-1}, 1644.2 cm^{-1}, and 1543.9 cm^{-1}, representing N—H bonding stretching vibration, C—O stretching vibration, and C—N stretching vibration, respectively (Song, Guo, et al., 2024). After noncovalent binding with flavonoids and ultrasound treatment (Fig. 4B), the position and intensity of the characteristic absorption peak of β-LG - flavonoids complexes changed compared with β-LG. In addition, the characteristic peaks of each complex shifted, indicating that the binding degree between β-LG and flavonoids was different. Our results were similar with the reported research. Ma and Zhao (2019) found that the absorption peaks of whey protein isolate (WPI) - galangin and WPI – genistein complexes showed different degrees of redshift near the amide I and II bands, which indicated the difference in the binding degree between WPI and polyphenols (Ma & Zhao, 2019).

Intrinsic fluorescence quenching spectra is applied to evaluated the interaction between the protein and polyphenols commonly, which can provide information about the microenvironment of the chromophores in protein molecules. In this study, fluorescence quenching analysis was used to unveil the possible effect of ultrasound on the modification of β-LG - flavonoids interactions. The protein intrinsic fluorescence is induced mainly by the fluorescence emission of phenylalanine (Phe),

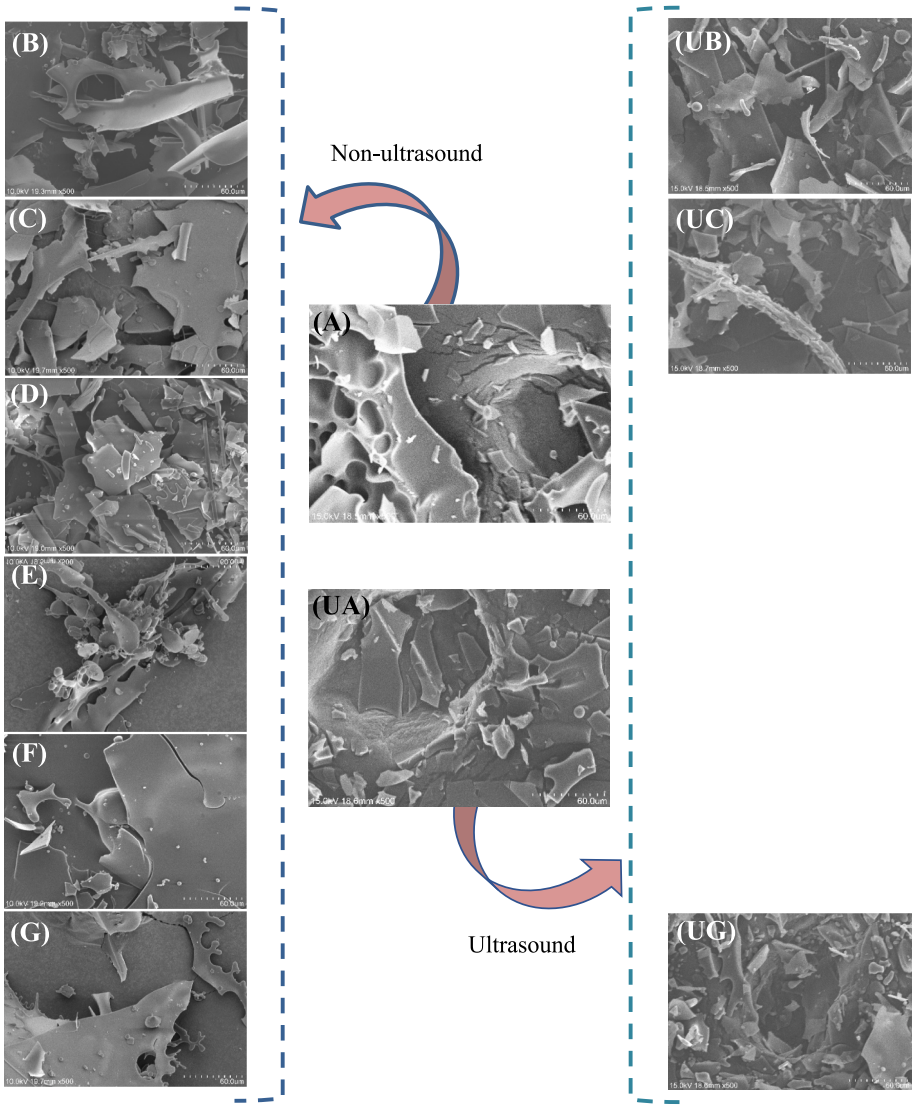

Fig. 2. SEM of different samples before (A to G) and after (UA to UG) ultrasound treatment. (A, UA: β-LG; B, UB: β-LG-API complex; C, UC: β-LG-AGL complex; D, UD: β-LG-LUT complex; E, UE: β-LG-LGL complex; F, UF: β-LG-MY complex; G, UG: β-LG-MYR complex).

tryptophan (Trp), and tyrosine (Tyr) residues when excited at 280 nm (Vivian & Callis, 2001). The reduction in the protein fluorescent intensity means certain quencher-fluorophore interactions, reflects the change of Trp residue environment and the protein tertiary structure (Liang et al., 2023). The fluorescence spectra of samples before and after ultrasound treatment were shown in Fig. 4C and D. The maximum emission wavelength (λ_{max}) of the native β-LG could be observed at 337 nm, being characteristic of Trp emission. Ultrasound treatment affected the emission spectra of β-LG. Ultrasound decreased the fluorescent intensity of β-LG ascribed to protein conformational rearrangement and exposure of chromophore groups to solvent, which changed the polarity of the environment (Pan et al., 2020). In addition, the intermolecular aggregation induced by a combined effect of ultrasonic actions and noncovalent binding could decrease the fluorescence intensity of the complex. After ultrasound treatment and noncovalent binding, a notable red-shifting in the λ_{max} of all samples was observed, indicating that flavonoids-interaction and ultrasound modified the polypeptide backbone of proteins, inducing the microenvironment of Trp residues to more polar region and being capable to interact with water molecules (Zhang, Lu, et al., 2021). Liu et al. found that the interaction of flavonoids (epigallocatechin gallate, quercetin, apigenin, naringenin) and WPI could significantly reduce the endogenous fluorescence intensity of proteins. The most fluorescence quenching ability among these four polyphenols on WPI was epigallocatechin gallate, followed by apigenin, naringin, and quercetin, which indicated that the structural difference of flavonoids can affect the fluorescence quenching ability of flavonoids (Liu et al., 2021). The quenching mechanism is described by the Stern-Volmer equation: $\frac{F_0}{F} = 1 + Kq\tau_0[Q] = 1 + Ksv$. Where the F_0 and F represent the protein fluorescence concentrations before and after the addition of the quencher (API, LUT, MY, AGL, LGL, MYR). The symbol [Q] indicates the concentration of the added quencher. Ksv denotes the Stern-Volmer quenching constant, Kq is the quenching rate constant, and τ_0 represents the average lifetime of the biomolecule in the absence of the quencher. As shown in Table 1, the biomolecular quenching rate constant Kq is significantly greater than the maximum diffusive collisional quenching constant (2.0×10^{10} M^{-1}). This indicates that the quenching of β-Lg fluorescence by API, LUT, MY, AGL, LGL, and MYR occurs through a static quenching mechanism (Zhu et al., 2020).

CD spectroscopy is a sensitive, easy, and fast technology, which is commonly used to reveal the variation in the secondary structure of proteins. The secondary structural profile of β-LG affected by flavonoids binding and ultrasound treatment could be analyzed by CD spectroscopy. As depicted in Fig. 3E and F, the measurement range was from 190 to 260 nm. The positive and negative peaks at 193 nm and 208–210 nm

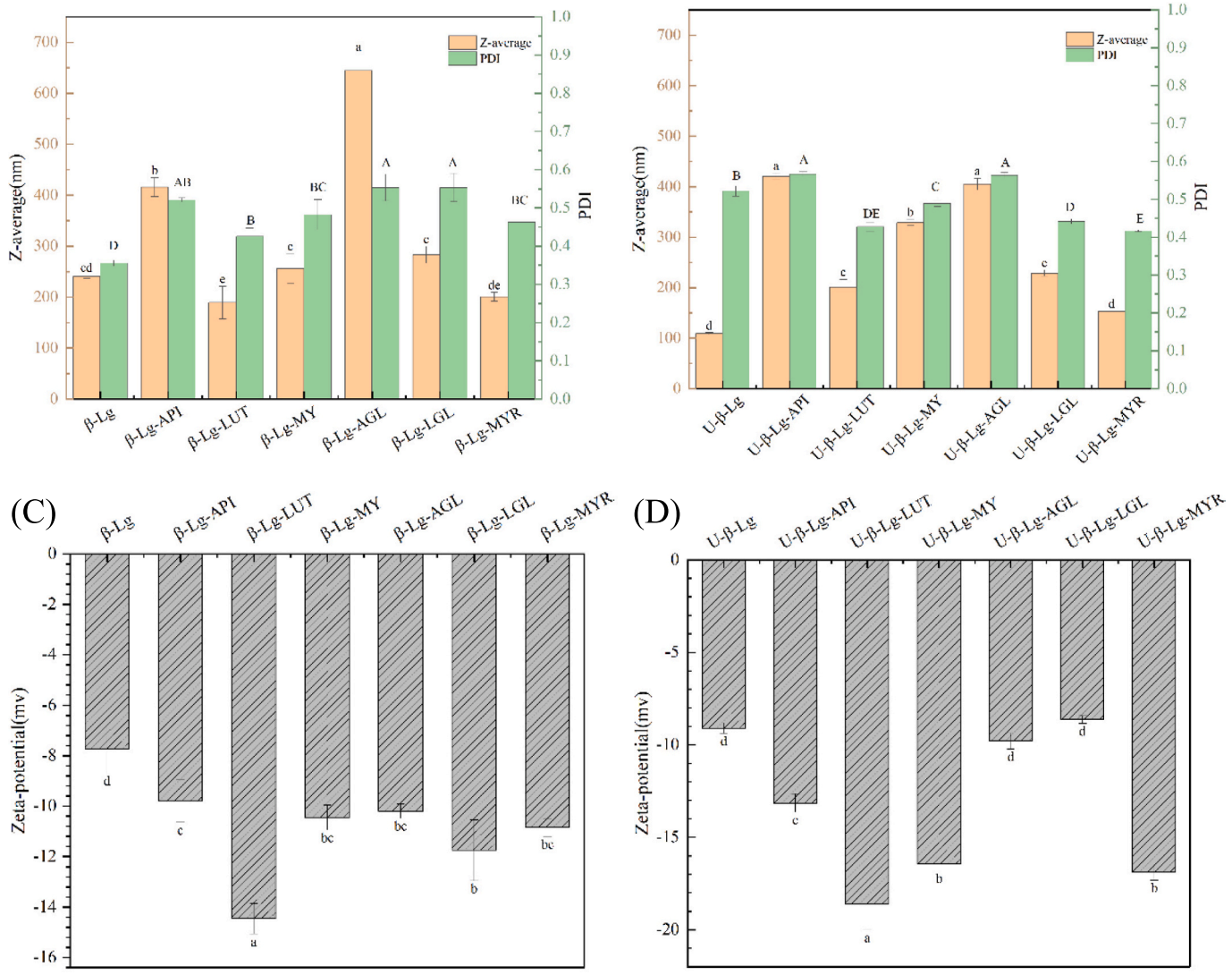

Fig. 3. Particle size and potential of β-LG and β-LG - flavonoids complexes: (A) particle size of the control group; (B) particle size of the ultrasound group; (C) zeta potential of the control group; (D) zeta potential of the ultrasound group.

correspond to the characteristic of a α-helical structure. The β-sheet structure can be detected in the positive peak at 195 nm and the negative peak at 215–220 nm (Song et al., 2025). As shown in Table S1, the contents of the secondary structures detected in the native β-LG were as follows: 12.1 % α-helix, 33.7 % β-sheet, 41.6 % β-turn, and 12.6 % random coil. After binding API, AGL, LUT, LGL, MY, and MYR, the α-helix contents were decreased to 13.1 %, 17.0 %, 25.0 %, 13.8 %, 13.2 %, and 12.8 %, respectively. After ultrasound treatment, the α-helix contents almost doubled. By a combined effect of ultrasonic actions and noncovalent binding, the contents of the β-sheet structure and the random coil increase slightly, while the β-turn structure content decreased significantly ($P < 0.05$). The result revealed that the secondary structure modifications of β-LG induced by binding of six flavonoids and ultrasound. Zhang et al. demonstrated that pre-sonication could induce a greater extent of β-LG structural rearrangement. It was beneficial for the hydrophobic stacking interaction between flavonoids and β-LG using ultrasound. Because of specific binding locations, the formation mode of β-LG was essential for the spatial structure of the complex (Zhang, Lu, et al., 2021).

For predicting the lowest state of receptor-ligand molecule interactions and the optimal conformation for noncovalent binding between proteins and flavonoids molecules, molecular docking considered as a computer-aided technology was used. Considering the schematic diagram of molecular docking (Fig. 5), it can be observed that the six types of flavonoids primarily interact with the outer surface of β-LG. This observation aligns with the findings of Li et al., who reported that flavonoid ligands bind to the outer surface of β-LG rather than the central calyx (Li et al., 2018). As shown in Fig. 5A, the most favorable binding conformation with the most negative score (−6.5 kcal/mol) of API was surrounded by 7 residues. These main residues composed of the binding pocket of β-LG. Some hydrophobic residues (e.g. Val-43, Phe-105, Leu-39, and Asn-90) constituted the hydrophobic cavity. With a negative charge residue Asn-90, API formed two hydrogen bonds by the hydroxyl group acting as both hydrogen bond acceptor and donor on the B ring (Liang et al., 2023; Shen et al., 2022). We found that LUT bound to β-LG amino acid residues (Asn-90, Ala-86, Ile-72, and Ile-71) via hydrogen bonds with the most negative score (−6.0 kcal/mol). Moreover, MY also interacted with Asn-88, Asn-90, Glu-89, Ala-86, Val-41, and Leu-58 via hydrophobic interactions. These results were in line with the reported research hydrophobic forces and hydrogen bonding dominated the interactions involved in protein-flavonoid noncovalent binding (Liang et al., 2023). After glycosylation reaction, AGL interacted with Ile-56, Val-43, Val-92, Phe-105, and Leu-58 by hydrophobic interaction with the most negative score (−7.0 kcal/mol). For LGL, six hydrophobic residues (Val-41、Ile-56、Leu-39、Ile-84、Leu-58 and Ile-71) played dominant roles in maintaining the conformations of β-LG-

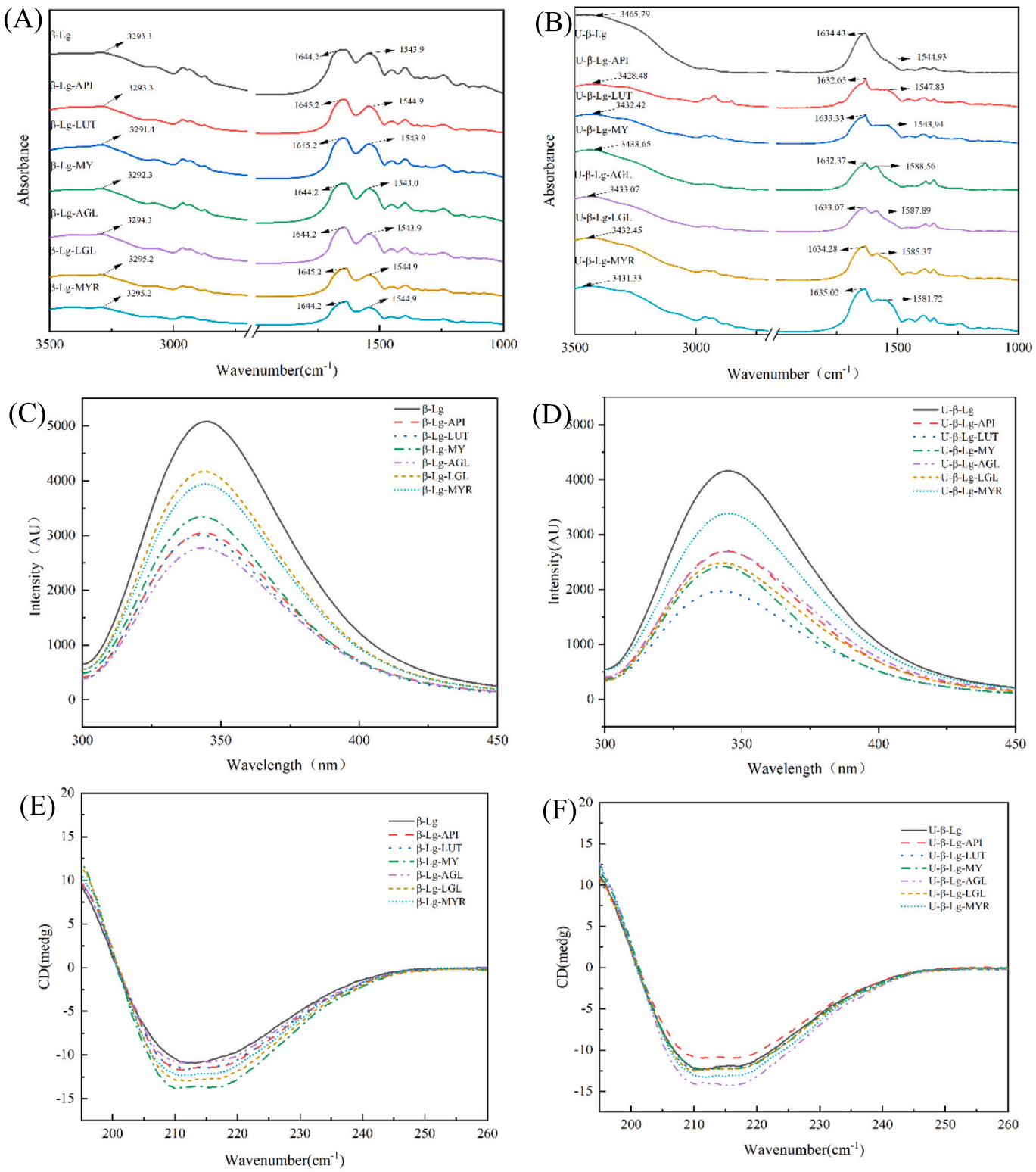

Fig. 4. FTIR, fluorescence spectroscopy, and CD spectroscopy of β-LG and β-LG - flavonoids complexes before (A, C, E) and after (B, D, F) ultrasound treatment. (A, C, E: control groups; B, D, F: ultrasound groups).

LGL complex by the binding interaction with the most negative score (−6.8 kcal/mol). Furthermore, MYR also interacted with Ile-71、Ile-84, and Ala-86 by hydrophobic interaction, which could strengthen the van der Waals forces between proteins and flavonoids with the most negative score (−6.8 kcal/mol). Our results demonstrated that hydrophobic interactions and hydrogen bonding promoted stabilization of flavonoid ligands within the binding cavity of β-LG. In addition, compared with the binding affinity constants among these complexes, the binding capability of β-LG-AGL was the most.

3.4. Changes in functional properties

The protein structure changes are commonly accompanied by variations in the protein thermal property. The transition temperature (Ts)

Table 1
Comparison of thermal stability, surface hydrophobicity, and antioxidant activity of β-LG bound to flavonoids with or without ultrasound treatment.

Sample	T_S (°C)	ΔH(J/g)	H_0 (slope x 10^2)	DPPH	ABTS	FARP
				(μmol Trolox/g sample)		
β-LG	81.4	179.9	2362.3 ± 2.17^{a}	60.9 ± 1.10^{f}	160.7 ± 8.92^{e}	6.8 ± 0.87^{e}
β-LG-API	90.0	181.5	1259.2 ± 3.75^{b}	69.3 ± 0.93^{d}	481.9 ± 7.77^{d}	12.4 ± 0.57^{d}
β-LG-LUT	85.9	216.5	1230.7 ± 2.27^{c}	78.8 ± 1.26^{c}	518.0 ± 16.05^{c}	34.5 ± 3.77^{b}
β-LG-MY	93.6	192.3	1188.3 ± 7.68^{d}	86.0 ± 0.65^{a}	626.1 ± 8.17^{a}	37.6 ± 3.27^{ab}
β-LG-AGL	86.3	183.6	1188.0 ± 2.42^{d}	68.2 ± 0.42^{e}	471.6 ± 5.35^{d}	11.5 ± 2.41^{de}
β-LG-LGL	85.0	184.2	1102.0 ± 4.95^{e}	78.8 ± 0.96^{c}	483.0 ± 9.93^{d}	20.8 ± 1.63^{c}
β-LG-MYR	91.3	187.7	965.8 ± 6.87^{f}	79.7 ± 0.25^{b}	580.8 ± 10.85^{b}	41.0 ± 3.27^{a}
U-β-LG	83.0	184.3	2259.9 ± 2.69^{a}	67.2 ± 0.72^{g}	174.1 ± 9.44^{e}	9.5 ± 0.75^{g}
U-β-LG-API	92.7	193.1	1224.3 ± 1.47^{b}	72.6 ± 0.56^{e}	607.5 ± 12.35^{cd}	19.5 ± 0.94^{e}
U-β-LG-LUT	98.9	252.3	992.6 ± 1.00^{d}	89.2 ± 0.64^{b}	623.0 ± 14.15^{bc}	42.4 ± 1.32^{c}
U-β-LG-MY	97.3	235.6	977.0 ± 3.95^{d}	91.6 ± 1.18^{a}	652.8 ± 4.72^{a}	52.0 ± 1.30^{a}
U-β-LG-AGL	92.4	188.9	1155.6 ± 6.58^{c}	69.4 ± 0.94^{f}	594.2 ± 9.93^{d}	15.6 ± 0.78^{f}
U-β-LG-LGL	86.8	191.6	923.5 ± 5.84^{e}	81.5 ± 1.55^{d}	611.7 ± 7.73^{cd}	39.9 ± 1.35^{d}
U-β-LG-MYR	91.3	225.7	725.6 ± 8.90^{f}	84.2 ± 0.60^{c}	635.3 ± 6.18^{ab}	46.1 ± 0.22^{b}

Note: different letters in superscript within the same row indicate significant differences among samples ($p < 0.05$).

and enthalpy change (ΔH) associated with the thermal denaturation of β-LG were measured by DSC. Ts and ΔH values reflect the thermal stability and the energy required to unfold the protein (Song, Zeng, et al., 2024). Protein denaturation is an endothermic process, which mainly includes the dissociation of intramolecular bonds such as the breakage of noncovalent bond (Sun et al., 2019). As shown in Table 1, the Ts values of β-LG and Uβ-LG were 81.4 °C and 83.0 °C, respectively. This may be due to the fact that ultrasound promoted the unfolding of the protein structure. The similar research has been demonstrated (Kanakis et al., 2011). After the noncovalent binding with flavonoids, the Ts values of six complexes all increased significantly ($P < 0.05$). Furthermore, the Ts values further increased after ultrasound treatment. This result demonstrated that the physical attachment of flavonoids to the protein molecules enhanced the thermal stability. Similar to the change in Ts, ΔH values of all samples increased by a combined effect of noncovalent binding and ultrasonic actions. This meant more energies were required to unfold the protein structure during the noncovalent interaction between β-LG and flavonoids. On the other hand, ultrasound may cause the protein to fold, forming new intramolecular or intermolecular bonds in the protein. The important forces applied to maintain the conformation of the protein are the hydrogen bonding, hydrophobic, electrostatic, and disulfide interactions. Sun et al. reported that proper ultrasound treatment could promote the protein thermal stability effectively (Sun et al., 2019).

The surface hydrophobicity is commonly used to reveal variations in protein conformation that affect functional properties, which plays a crucial role on the interfacial properties of involved proteins. The fluorescence intensity of a common fluorescence probe ANS was measured from the H_0 value to evaluate the effects of ultrasonic actions and noncovalent binding on the surface hydrophobicity of β-LG. The fluorescence emitted by free ANS in aqueous solution is weak extremely, while the quantum yield on binding to the hydrophobic regions on proteins increased significantly (Liang et al., 2023; Zhu et al., 2020). As shown in Table 1, the H_0 value of β-LG decreased after ultrasound treatment, which demonstrated that ultrasound could expand the molecule structure of proteins and expose more hydrophilic groups to the polar environment. By a combined effect of noncovalent binding and ultrasonic actions, H_0 values of complexes were all decreased. This revealed that the hydrophobic solvent accessibility of β-LG decreased, which may be due to the blocking of hydrophobic regions on the protein surface by ligands by noncovalent binding. Liang et al. suggested that another reason for the decrease of protein surface hydrophobicity was that the addition of flavonoids induced the protein aggregation (Liang et al., 2023). Similar results have been reported (Dai et al., 2022). Among six β-LG-flavonoid complexes, H_0 values of AGL, LGL, and MYR were lower than those of API, LUT, and MY. Because the glucoside bond belongs to the hydrophilic group, which can promote the hydration of proteins.

ABTS, DPPH, and FRAP assays were used to evaluate the effect of flavonoids conjugation and ultrasound on the antioxidant property of β-LG. ABTS and DPPH are based on an electron transfer and involves reduction of a colored oxidant. It has been found that DPPH and ABTS are both nonphysiologically and artificial relevant radicals, which meant only direct reactions of the investigated antioxidant compounds with the radical were measured (Rumpf et al., 2023). The FRAP assay is different from the others as there are no free radicals involved but the reduction of ferric iron (Fe^{3+}) to ferrous iron (Fe^{2+}) is monitored. The presence of an antioxidant can induce the reduction of iron ions, causing the change of color. The advantages of this assay were high precision and sensitivity. The three assays both relied on a single electron transfer mechanism. The different reaction mechanism reflected different antioxidative attributes (Rumpf et al., 2023). As shown in Table 1, the ability of β-LG to scavenge DPPH radicals was equivalent to 60.91 μmol Trolox/g. After noncovalent binding with flavonoids, the antioxidant ability of the complex all increased. After ultrasound treatment, the antioxidant ability further enhanced. This revealed that the noncovalent interaction between β-LG and flavonoids under ultrasound could form more stable complexes, which could scavenge free radicals and ultimately terminated the free radical chain reaction. Among six complexes, the DPPH scavenging ability of β-LG-MYR was the strongest, which may be due to the maximum number of phenolic hydroxyl groups in MYR. It has been reported that more hydroxyl groups can promote better electron donating effect of protein – flavonoid complexes (Zhang, Lu, et al., 2021). The ability of β-LG to scavenge ABTS radicals was equivalent to 137.03 μmol Trolox/g. The value of β-LG increased to 174.10 μmol Trolox/g after ultrasound. This is mainly due to the formation of numerous hydroxyl radicals during ultrasound process, which can promote the protein hydroxylation. In addition, ultrasound can also unfold the compact spherical structure, change the secondary and tertiary structures of proteins (Pan et al., 2023). Compared to three protein-flavonoids (β-LG-API, β-LG-LUT, and β-LG-MY) complexes, the ABTS scavenging ability of β-LG-AGL, β-LG-LGL, and β-LG-MYR were lower. The result revealed that glycosylation would reduce the ABTS scavenging ability, which was because that the large steric hindrance in the glucoside bond reduced the binding of flavonoids to proteins. The result of the ferric reducing power was similar to those of DPPH and ABTS radical scavenging assays. These results demonstrated all three assays were efficient to determine the antioxidant ability of β-LG-flavonoid complexes, the antioxidant ability could be improved by a combined effect of noncovalent binding and ultrasonic actions, and the correlation between the antioxidant ability and the number of phenolic hydroxyl groups and the binding amounts of flavonoids.

3.5. Analysis of the potential for LY delivering

In this study, the characterization and physicochemical properties of six binary complexes have carried out. Results have demonstrated that the thermal stability, surface hydrophilicity, and antioxidant properties of three protein-flavonoids (β-LG-API, β-LG-LUT, and β-LG-MY)

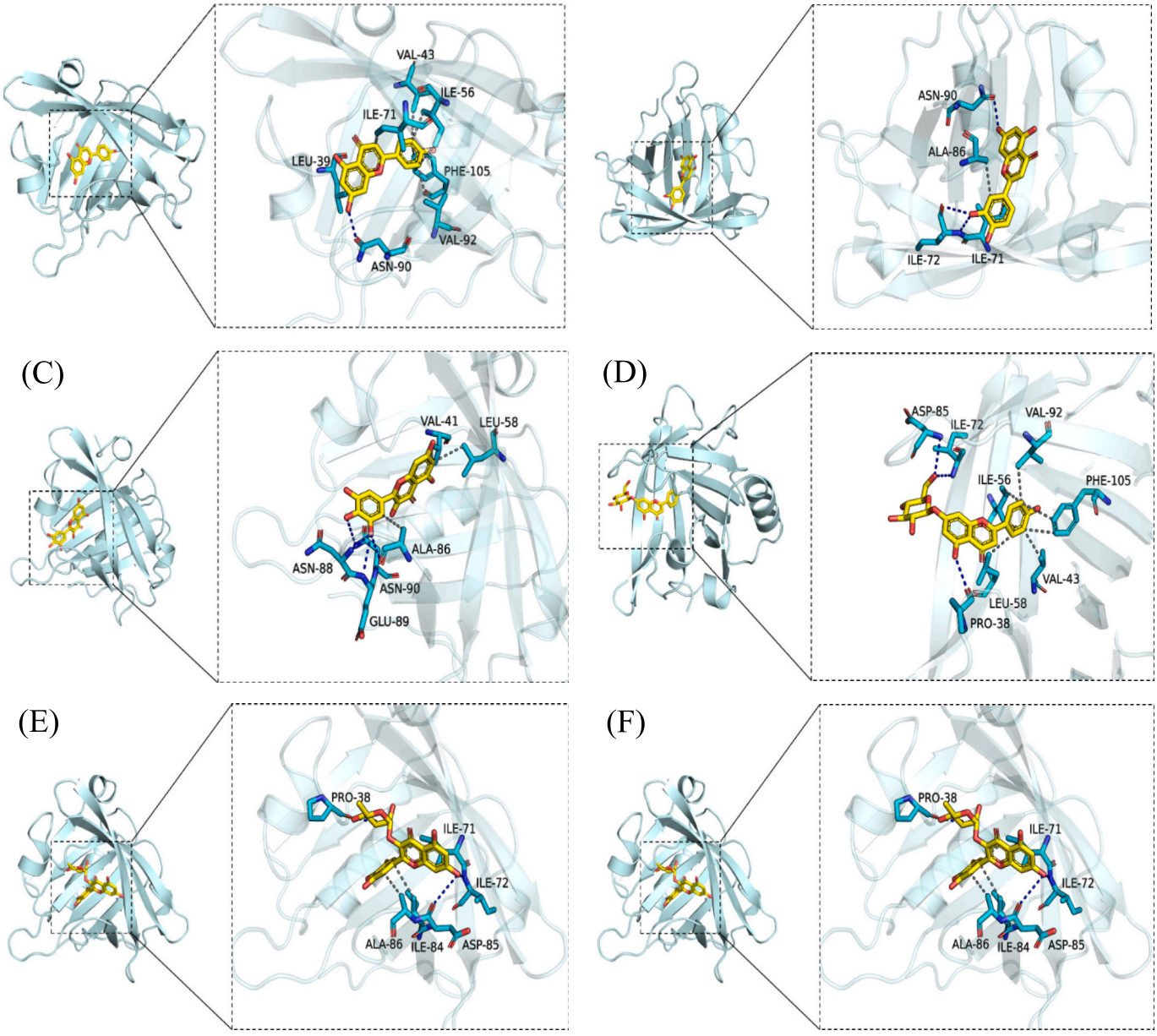

Fig. 5. The binding mode of β-LG - flavonoids complexes based on molecular docking: (A) β-LG-API; (B) β-LG-LUT; (C) β-LG-MY; (D) β-LG-AGL; (E) β-LG-LGL; (F) β-LG-MYR. (Note: the left figure was the overall view, and the right figure was the local view. In figures, the yellow stick represents the small molecule, the cyan cartoon represents the β- lactoglobulin, the blue line represents the hydrogen bonding, and the gray line represents the hydrophobic interaction). (For interpretation of the references to color in this figure legend, the reader is referred to the web version of this article.)

complexes were superior. To expand the application of these complexes, the characterization and stability for LY delivering were investigated systematically. As shown in Fig. S1, β-Lg encapsulated lycopene at a rate of 48.17 %. Furthermore, the complex system's encapsulation efficiency increased by 15.15 %, reaching 37.59 % when the β-Lg-flavonoid complex encapsulated lycopene compared to β-Lg alone. Among them, β-Lg-MY exhibited the highest capacity for loading lycopene. This enhanced ability may be attributed to the presence of the most phenolic hydroxyl groups in MY, which facilitate the formation of hydrogen bonds with lycopene. In addition, the phenolic hydroxyl group may influence the intermolecular hydrophobic interactions of the complexes, thereby enhancing the affinity between the complexes and lycopene. This results in a tighter binding of lycopene within the embedding system.

In Fig. 6A, the characteristic peak of LY was detected. The sharp band at 960.0 cm^{-1} is attributed to the absorption of -C-C- of the polyene chain of LY (Gu et al., 2023). The characteristic peak of LY was disappeared after loaded, which revealed that LY could occupied the helical cavity of proteins and protein-flavonoid complexes, the cavity hid the characteristic absorption of LY, and the protein-flavonoid-LY complex was formed. The XRD result was shown in Fig. 6B. It presented six characteristic peaks ($2\theta = 14.8°, 16.0°, 17.2°, 21.7°, 24.1°$, and $25.7°$) of LY (Gu et al., 2023). The disappeared characteristic peaks further demonstrated LY was encapsulated within the helical cavity of proteins and the complex. It has been reported that the conformation of β-LG commonly changed (e.g. dimer-to-monomer dissociation below pH 3.0, and tanford transition above pH 7.0) at different pH levels, which can affect the ligand-binding properties (Zhou et al., 2024). As shown in Fig. 6C, protein-flavonoid-LY complexes at pH 4 and 6 had lower particle sizes substantially compared to other complexes ($P < 0.05$), suggesting the larger cover of hydrophobic patches by LY. It was found that protein aggregation was affected by these hydrophobic patches seriously

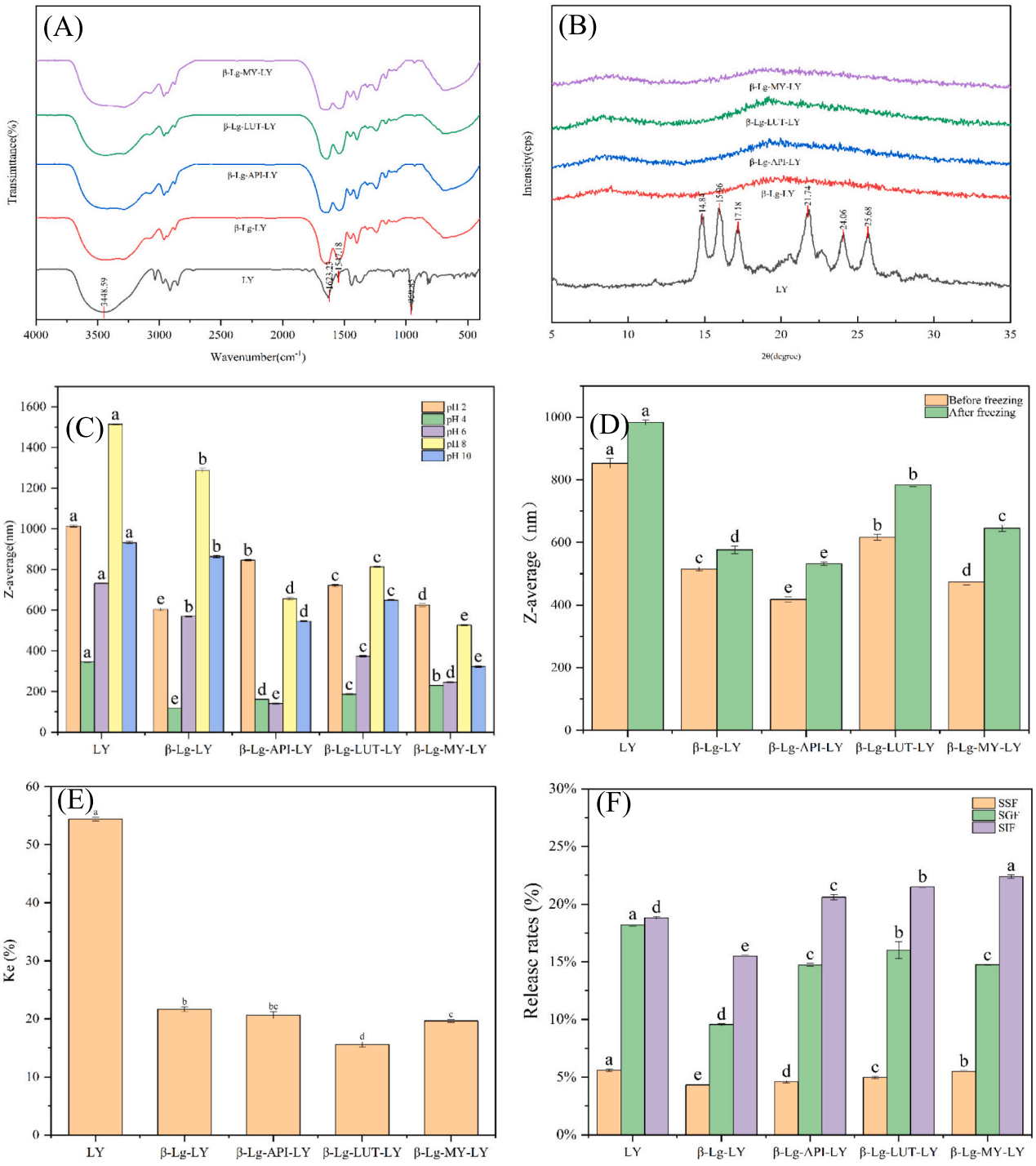

Fig. 6. Analysis of the potential for LY delivering. (A) FTIR spectra; (B) XRD spectra; (C) pH stability; (D) freeze stability; (E) centrifuge stability; (F) Release rate.

(Wang et al., 2021). Among all samples, the β-LG-API-LY complex showed less variation in particle size, indicating the best pH stability.

After freezing, the particle size of complexes enlarged (Fig. 6D). This is mainly because the exchange of LY crystals promoted partial coalescence of complexes. β-LG loaded with LY after flavonoid modification could enhance the freezing stability of the ternary complex. The β-LG-API-LY complex showed the best freeze stability. As showed in Fig. 6E, the centrifugal stability values (Ke) of the complex decreased significantly after centrifugation for sample solutions ($P < 0.05$). The result revealed that the binary complex embedded LY had better centrifugal stability than the pure protein. The β-LG-LUT-LY complex had the best centrifugal stability. As illustrated in the Fig. S2, the retention of lycopene under UV light irradiation gradually decreased with increasing treatment time. This is because lycopene contains several unsaturated double bonds, which makes it sensitive to light. However, the retention of lycopene in the complex was significantly higher than that in the control group. The retention of LY after 2 h of UV treatment decreased by approximately 16 %, while the maximum decrease of the complex was only about 8 %. The retention of LY and its complexes after 12 h of UV irradiation has nearly reached a minimum level, with little to no difference in retention observed in samples treated for 24 h. The highest retention of LY was observed in β-Lg-MY-LY. This may be attributed to the strong antioxidant activity provided by MY, which effectively quenches the free radicals generated by light, thereby preventing the

oxidation and degradation of lycopene (Wang et al., 2021). After digestion, the ternary complex stabilized by protein was destroyed by digestive juices. The bio-accessibility of LY was expressed by measuring the release rate of LY in the digesta. As depicted in Fig. 6F, the bio-accessibility of LY was impacted significantly by modified β-LG with API, LUT, and MY conjugate. LY undergoes oral digestion without a significant change in the rate of complex release. During the gastric digestion phase, the acidic environment, characterized by a low pH and pepsin, causes partial denaturation of proteins, resulting in a slight release of encapsulated LY into the gastric digestion. In addition, the presence of flavonoids may stabilize the structure of the complexes, thereby slowing the rate of LY digestion in the stomach. When the complexes enter the small intestine, the release of LY is hindered by the presence of pancreatic enzymes and bile. This phenomenon occurs because trypsin can disrupt the structure of the complex, leading to the further release of LY encapsulated within it, thereby enhancing the bioaccessibility of LY. The β-LG-API-LY complex had the best bio-accessibility, which could be applied for controlled release of LY in the food industry.

4. Conclusions

In this study, the potential effect of ultrasound treatment on non-covalent interactions between β-LG and three flavonoids (API, LUT, and MY) and their corresponding glycosylated derivatives (AGL, LGL, and MYR) was investigated. Results revealed that ultrasound treatment promoted reactive groups exposure and structural unfolding of β-LG to interact with six flavonoids. By a static quenching mechanism driven by hydrophobic interactions, API, LUT, MY, AGL, LGL, and MYR could all bind with β-LG via noncovalent interaction. The docking results showed that the preferred binding site for these flavonoids was on the outer surface of β-LG. The thermal stability, surface hydrophilicity, and anti-oxidant properties of β-LG were significantly improved by noncovalent binding with flavonoids and ultrasound treatment ($P < 0.05$). In addition, the β-LG-API, β-LG-LUT, and β-LG-MY complexes exhibited favorable potential for delivering LY. The ability of the β-LG-API to deliver LY was the best, and it could enhance the freeze stability, centrifuge stability, thermal stability, and pH stability of the system significantly. It will be essential to study more comprehensive mechanisms of non-covalent interaction between β-LG and flavonoids, assess the effect of ultrasound and noncovalent interaction on the bioactivity, stability and bioavailability on β-LG-flavonoid complexes, and design a more promising delivery system for LY based on β-LG- flavonoid complexes in future research.

Ethical approval

There were no any studies on human participants contained in this article. All applicable guidelines followed for the use and care of animals were institutional, national, and international.

CRediT authorship contribution statement

Gongshuai Song: Writing – review & editing, Writing – original draft. **Fang Li:** Methodology, Investigation. **Ziming Xu:** Writing – review & editing. **Nengliang Jiang:** Software. **Danli Wang:** Formal analysis. **Tinglan Yuan:** Visualization. **Ling Li:** Visualization. **Jinyan Gong:** Supervision, Funding acquisition.

Declaration of competing interest

The authors declare that they have no known competing financial interests or personal relationships that could have appeared to influence the work reported in this paper.

Acknowledgement

This work was supported by the National Natural Science Foundation of China (32372469 and 31871763), Zhejiang Provincial Natural Science Foundation of China (LZ24C200006), Zhejiang Province Key Science and Technology Projects (2023C02045 and 2024C04020), and Qianjiang Special Expert Project of Hangzhou.

Appendix A. Supplementary data

Supplementary data to this article can be found online at https://doi.org/10.1016/j.fochx.2025.102160.

Data availability

Data will be made available on request.

References

Alizadeh-Pasdar, N., & Li-Chan, E. C. (2000). Comparison of protein surface hydrophobicity measured at various pH values using three different fluorescent probes. *Journal of Agricultural and Food Chemistry, 48*(2), 328–334. https://doi.org/10.1021/jf990393p

Dai, S., Lian, Z., Qi, W., Chen, Y., Tong, X., Tian, T., Lyu, B., Wang, M., Wang, H., & Jiang, L. (2022). Non-covalent interaction of soy protein isolate and catechin: Mechanism and effects on protein conformation. *Food Chemistry, 384*, Article 132507. https://doi.org/10.1016/j.foodchem.2022.132507

Fu, M., Gao, L., Geng, Q., Li, T., Dai, T., Liu, C., & Chen, J. (2023). Noncovalent interaction mechanism and functional properties of flavonoid glycoside-β-lactoglobulin complexes. *Food & Function, 14*(3), 1357–1368. https://doi.org/10.1039/d2fo02791g

Gao, Q., Chen, J., Zhou, G., & Xu, X. (2023). Different protein-anthocyanin complexes engineered by ultrasound and alkali treatment: Structural characterization and color stability. *Food Chemistry, 427*, Article 136693. https://doi.org/10.1016/j.foodchem.2023.136693

Gu, T., Zhang, X., Gong, Y., Zhang, T., Hu, L., Yu, Y., Deng, C., Xiao, Y., Zheng, M., & Zhou, Y. (2023). An investigation into structural properties and stability of debranched starch-lycopene inclusion complexes with different branching degrees. *International Journal of Biological Macromolecules, 233*, Article 123641. https://doi.org/10.1016/j.ijbiomac.2023.123641

Guan, H., Zhang, W., Sun-Waterhouse, D., Jiang, Y., Li, F., Waterhouse, G. I. N., & Li, D. (2021). Phenolic-protein interactions in foods and post ingestion: Switches empowering health outcomes. *Trends in Food Science & Technology, 118*, 71–86. https://doi.org/10.1016/j.tifs.2021.08.033

Jia, Y., Fu, Y., Man, H., Yan, X., Huang, Y., Sun, S., Qi, B., & Li, Y. (2022). Comparative study of binding interactions between different dietary flavonoids and soybean β-conglycinin and glycinin: Impact on structure and function of the proteins. *Food Research International, 161*, Article 111784. https://doi.org/10.1016/j.foodres.2022.111784

Jin, C., Chu, C., Zhu, X., Lu, Y., Yu, N., Ye, Q., … Meng, X. (2024). Fractional extraction phenolics from *C. Oleifera* seed kernels exhibited anti-inflammatory effect *via* PI3K/Akt/NF-κB signaling pathway under Caco-2/RAW264.7 co-culture cell model. *Food Research International, 197*, Article 115268. https://doi.org/10.1016/j.foodres.2024.115268

Kanakis, C. D., Hasni, I., Bourassa, P., Tarantilis, P. A., Polissiou, M. G., & Tajmir-Riahi, H.-A. (2011). Milk β-lactoglobulin complexes with tea polyphenols. *Food Chemistry, 127*(3), 1046–1055. https://doi.org/10.1016/j.foodchem.2011.01.079

Leong, T., Juliano, P., & Knoerzer, K. (2017). Advances in ultrasonic and Megasonic processing of foods. *Food Engineering Reviews, 9*(3), 237–256. https://doi.org/10.1007/s12393-017-9167-5

Li, E., Wang, T., Zhou, R., Zhou, Z., Zhang, C., Wu, W., & He, K. (2021). Myricetin and myricetrin alleviate liver and colon damage in a chronic colitis mice model: Effects on tight junction and intestinal microbiota. *Journal of Functional Foods, 87*, Article 104790. https://doi.org/10.1016/j.jff.2021.104790

Li, T., Hu, P., Dai, T., Li, P., Ye, X., Chen, J., & Liu, C. (2018). Comparing the binding interaction between *β*-lactoglobulin and flavonoids with different structure by multi-spectroscopy analysis and molecular docking. *Spectrochimica Acta Part A: Molecular and Biomolecular Spectroscopy, 201*, 197–206. https://doi.org/10.1016/j.saa.2018.05.011

Li, X., Tu, Z., Qi, W., Wang, H., Yang, W., & Tian, M. (2016). Effect of ultrasound treatment on structure and antigenicity of β-lactoglobulin. *Science and Technology of Food Industry, 18*, 106–110 (in Chinese) 10.13386/j.issn1002-0306.2016.18.012.

Liang, F., Shi, Y., Shi, J., & Cao, W. (2023). Exploring the binding mechanism of pumpkin seed protein and apigenin: Spectroscopic analysis, molecular docking and molecular dynamics simulation. *Food Hydrocolloids, 137*, Article 108318. https://doi.org/10.1016/j.foodhyd.2022.108318

Lin, L.-C., Pai, Y.-F., & Tsai, T.-H. (2015). Isolation of Luteolin and Luteolin-7-O-glucoside from Dendranthema morifolium Ramat Tzvel and their pharmacokinetics in rats. *Journal of Agricultural and Food Chemistry, 63*(35), 7700–7706. https://doi.org/10.1021/jf505848z

Liu, J., Song, G., Yuan, Y., Zhou, L., Wang, D., Yuan, T., … Gong, J. (2022). Ultrasound-assisted assembly of β-lactoglobulin and chlorogenic acid for non covalent nanocomplex: Fabrication, characterization and potential biological function. *Ultrasonics Sonochemistry, 86*, Article 106025. https://doi.org/10.1016/j.ultsonch.2022.106025

Liu, J., Song, G., Zhou, L., Yuan, Y., Wang, D., Yuan, T., Li, L., Yuan, H., Xiao, G., & Gong, J. (2023). Recent advances in the effect of ultrasound on the binding of protein-polyphenol complexes in foodstuff. *Food Frontiers, 4*(2), 721–732. https://doi.org/10.1002/fft2.221

Liu, X., Song, Q., Li, X., Chen, Y., Liu, C., Zhu, X., Liu, J., Granato, D., Wang, Y., & Huang, J. (2021). Effects of different dietary polyphenols on conformational changes and functional properties of protein–polyphenol covalent complexes. *Food Chemistry, 361*, Article 130071. https://doi.org/10.1016/j.foodchem.2021.130071

Ma, C.-M., & Zhao, X.-H. (2019). Depicting the non-covalent interaction of whey proteins with Galangin or Genistein using the multi-spectroscopic techniques and molecular docking. *Foods, 8*(9), 360. https://doi.org/10.3390/foods8090360

Meng, Y., Wei, Z., & Xue, C. (2023). Deciphering the interaction mechanism and binding mode between chickpea protein isolate and flavonoids based on experimental studies and molecular simulation. *Food Chemistry, 429*, Article 136848. https://doi.org/10.1016/j.foodchem.2023.136848

Pan, L., Chen, J., Fu, H., Wang, N., Zhou, J., Zhang, S., Lu, S., Dong, J., Wang, Q., & Yan, H. (2023). Effects of fabrication of conjugates between different polyphenols and bovine bone proteins on their structural and functional properties. *Food Bioscience, 52*, Article 102375. https://doi.org/10.1016/j.fbio.2023.102375

Pan, M., Xu, F., Wu, Y., Yao, M., Xiao, X., Zhang, N., Ju, X., & Wang, L. (2020). Application of ultrasound-assisted physical mixing treatment improves in vitro protein digestibility of rapeseed napin. *Ultrasonics Sonochemistry, 67*, Article 105136. https://doi.org/10.1016/j.ultsonch.2020.105136

Rumpf, J., Burger, R., & Schulze, M. (2023). Statistical evaluation of DPPH, ABTS, FRAP, and Folin-Ciocalteu assays to assess the antioxidant capacity of lignins. *International Journal of Biological Macromolecules, 233*, Article 123470. https://doi.org/10.1016/j.ijbiomac.2023.123470

Shafaei, Z., Ghalandari, B., Vaseghi, A., Divsalar, A., Haertlé, T., Saboury, A. A., & Sawyer, L. (2017). β-Lactoglobulin: An efficient nanocarrier for advanced delivery systems. *Nanomedicine: Nanotechnology, Biology and Medicine, 13*(5), 1685–1692. https://doi.org/10.1016/j.nano.2017.03.007

Shen, N., Wang, T., Gan, Q., Liu, S., Wang, L., & Jin, B. (2022). Plant flavonoids: Classification, distribution, biosynthesis, and antioxidant activity. *Food Chemistry, 383*, Article 132531. https://doi.org/10.1016/j.foodchem.2022.132531

Song, G., Guo, X., Li, Q., Lv, J., Wang, D., Yuan, T., … Gong, J. (2024). Mislabeling identification of fresh retail beef cuts using machine learning – Guided REIMS lipidomic fingerprints. *Food Control, 161*, Article 110401. https://doi.org/10.1016/j.foodcont.2024.110401

Song, G., Jiang, N., Ge, Y., Li, F., Zhou, L., Xiang, T., Wang, D., Yuan, T., Li, L., Luo, Z., & Gong, J. (2025). Improvement of curcumin loading properties and bioaccessibility of beta-lactoglobulin-hyaluronic acid nanocomplexes conjugated via ultrasound-assisted Maillard reaction. *International Journal of Biological Macromolecules, 288*, Article 138710. https://doi.org/10.1016/j.ijbiomac.2024.138710

Song, G., Zeng, M., Chen, S., Lyu, Z., Jiang, N., Wang, D., Yuan, T., Li, L., Mei, G., Shen, Q., & Gong, J. (2024). Exploring molecular mechanisms underlying changes in lipid fingerprinting of salmon (Salmo salar) during air frying integrating machine learning-guided REIMS and lipidomics analysis. *Food Chemistry, 460*, Article 140770. https://doi.org/10.1016/j.foodchem.2024.140770

Song, G., Zhou, L., Zhao, L., Wang, D., Yuan, T., Li, L., & Gong, J. (2024). Analysis of non-covalent interaction between β-lactoglobulin and hyaluronic acid under ultrasound-assisted treatment: Conformational structures and interfacial properties. *International Journal of Biological Macromolecules, 256*, Article 128529. https://doi.org/10.1016/j.ijbiomac.2023.128529

Sun, Q., Chen, Q., Xia, X., Kong, B., & Diao, X. (2019). Effects of ultrasound-assisted freezing at different power levels on the structure and thermal stability of common carp (Cyprinus carpio) proteins. *Ultrasonics Sonochemistry, 54*, 311–320. https://doi.org/10.1016/j.ultsonch.2019.01.026

Vivian, J. T., & Callis, P. R. (2001). Mechanisms of tryptophan fluorescence shifts in proteins. *Biophysical Journal, 80*(5), 2093–2109. https://doi.org/10.1016/S0006-3495(01)76183-8

Wang, C., Chen, L., Lu, Y., Liu, J., Zhao, R., Sun, Y., … Cuina, W. (2021). pH-dependent complexation between β-lactoglobulin and lycopene: Multi-spectroscopy, molecular docking and dynamic simulation study. *Food Chemistry, 362*, Article 130230. https://doi.org/10.1016/j.foodchem.2021.130230

Wang, H., Zhang, H., Liu, Q., Xia, X., Chen, Q., & Kong, B. (2022). Exploration of interaction between porcine myofibrillar proteins and selected ketones by GC-MS, multiple spectroscopy, and molecular docking approaches. *Food Research International, 160*, Article 111624. https://doi.org/10.1016/j.foodres.2022.111624

Wang, X., Li, W., Liu, J., He, Y., Meng, X., & Liu, B. (2024). Comparative study on encapsulation of four different flavonoids into pea protein isolate nanoparticles: The impact of glycosylation. *Journal of Molecular Liquids, 393*, Article 123571. https://doi.org/10.1016/j.molliq.2023.123571

Wu, D., Tang, L., Duan, R., Hu, X., Geng, F., Zhang, Y., Peng, L., & Li, H. (2021). Interaction mechanisms and structure-affinity relationships between hyperoside and soybean β-conglycinin and glycinin. *Food Chemistry, 347*, Article 129052. https://doi.org/10.1016/j.foodchem.2021.129052

Zhang, Q., Li, H., Cen, C., Zhang, J., Wang, S., Wang, Y., & Fu, L. (2021). Ultrasonic pre-treatment modifies the pH-dependent molecular interactions between β-lactoglobulin and dietary phenolics: Conformational structures and interfacial properties. *Ultrasonics Sonochemistry, 75*, Article 105612. https://doi.org/10.1016/j.ultsonch.2021.105612

Zhang, S., Li, X., Ai, B., Zheng, L., Zheng, X., Yang, Y., Xiao, D., & Sheng, Z. (2022). Binding of β-lactoglobulin to three phenolics improves the stability of phenolics studied by multispectral analysis and molecular modeling. *Food Chemistry: X, 15*, Article 100369. https://doi.org/10.1016/j.fochx.2022.100369

Zhang, Y., Lu, Y., Yang, Y., Li, S., Wang, C., Wang, C., & Zhang, T. (2021). Comparison of non-covalent binding interactions between three whey proteins and chlorogenic acid: Spectroscopic analysis and molecular docking. *Food Bioscience, 41*, Article 101035. https://doi.org/10.1016/j.fbio.2021.101035

Zhao, X., Wang, Z., Wu, G., Yin, L., Xu, L., Wang, N., & Peng, J. (2024). Apigenin-7-glucoside-loaded nanoparticle alleviates intestinal ischemia-reperfusion by ATF3/SLC7A11-mediated ferroptosis. *Journal of Controlled Release, 366*, 182–193. https://doi.org/10.1016/j.jconrel.2023.12.038

Zhou, L., Huang, Y., Wang, D., Yuan, T., Song, G., Gong, J., … Li, L. (2024). Microencapsulation of lactobacillus sakei and lactobacillus rhamnosus in whey protein isolate and sodium hyaluronate for potential food-grade probiotic delivery system. *Food Bioscience, 61*, Article 104784. https://doi.org/10.1016/j.fbio.2024.104784

Zhu, J., Li, K., Wu, H., Li, W., & Sun, Q. (2020). Multi-spectroscopic, conformational, and computational atomic-level insights into the interaction of β-lactoglobulin with apigenin at different pH levels. *Food Hydrocolloids, 105*, Article 105810. https://doi.org/10.1016/j.foodhyd.2020.105810

Zhu, Q., Qiu, Y., Zhang, L., Lu, W., Pan, Y., Liu, X., Li, Z., & Yang, H. (2024). Encapsulation of lycopene in Pickering emulsion stabilized by complexes of whey protein isolate fibrils and sodium alginate: Physicochemical property, structural characterization and in vitro digestion property. *Food Research International, 191*, Article 114675. https://doi.org/10.1016/j.foodres.2024.114675